Wei *et al. Molecular Cancer* (2024) 23:165
https://doi.org/10.1186/s12943-024-02075-y

Molecular Cancer

RESEARCH Open Access

Novel humanized monoclonal antibodies against ROR1 for cancer therapy

Rong Wei[1†], Xun Liao[1†], Jiao Li[1], Xiaoyu Mu[1], Yue Ming[1] and Yong Peng[1,2*]

Abstract

Background Overexpression of receptor tyrosine kinase-like orphan receptor 1 (ROR1) contributes to cancer cell proliferation, survival and migration, playing crucial roles in tumor development. ROR1 has been proposed as a potential therapeutic target for cancer treatment. This study aimed to develop novel humanized ROR1 monoclonal antibodies and investigate their anti-tumor effects.

Methods ROR1 expression in tumor tissues and cell lines was analyzed by immunohistochemistry and flow cytometry. Antibodies from mouse hybridomas were humanized by the complementarity-determining region (CDR) grafting technique. Surface plasmon resonance spectroscopy, ELISA assay and flow cytometry were employed to characterize humanized antibodies. In vitro cellular assay and in vivo mouse experiment were conducted to comprehensively evaluate anti-tumor activity of these antibodies.

Results ROR1 exhibited dramatically higher expression in lung adenocarcinoma, liver cancer and breast cancer, and targeting ROR1 by short-hairpin RNAs significantly inhibited proliferation and migration of cancer cells. Two humanized ROR1 monoclonal antibodies were successfully developed, named h1B8 and h6D4, with high specificity and affinity to ROR1 protein. Moreover, these two antibodies effectively suppressed tumor growth in the lung cancer xenograft mouse model, c-Myc/Alb-cre liver cancer transgenic mouse model and MMTV-PyMT breast cancer mouse model.

Conclusions Two humanized monoclonal antibodies targeting ROR1, h1B8 and h6D4, were successfully developed and exhibited remarkable anti-tumor activity in vivo.

Keywords ROR1, Humanized antibody, Specificity, Affinity

Introduction

Receptor tyrosine kinase-like orphan receptor 1 (ROR1) is a transmembrane glycoprotein, consisting of an extracellular immunoglobulin-like domain, a Frizzled domain (also called a cysteine-rich domain), a Kringle domain adjacent to the membrane, an intracellular tyrosine kinase domain and two serine/threonine-rich sections flanking a proline-rich domain [1]. ROR1 plays important roles in embryonic and fetal development and is found to be expressed at very low levels in human adult tissues [2]. Recently, elevated ROR1 expression was observed in different types of cancers, such as leukemia, lung cancer and

†Rong Wei and Xun Liao contributed equally to this work.

*Correspondence:
Yong Peng
yongpeng@scu.edu.cn
[1]Laboratory of Molecular Oncology, Frontiers Science Center for Disease-related Molecular Network, State Key Laboratory of Biotherapy and Cancer Center, West China Hospital, Sichuan University, Chengdu 610041, China
[2]Frontiers Medical Center, Tianfu Jincheng Laboratory, Chengdu 610212, China

© The Author(s) 2024. **Open Access** This article is licensed under a Creative Commons Attribution-NonCommercial-NoDerivatives 4.0 International License, which permits any non-commercial use, sharing, distribution and reproduction in any medium or format, as long as you give appropriate credit to the original author(s) and the source, provide a link to the Creative Commons licence, and indicate if you modified the licensed material. You do not have permission under this licence to share adapted material derived from this article or parts of it. The images or other third party material in this article are included in the article's Creative Commons licence, unless indicated otherwise in a credit line to the material. If material is not included in the article's Creative Commons licence and your intended use is not permitted by statutory regulation or exceeds the permitted use, you will need to obtain permission directly from the copyright holder. To view a copy of this licence, visit http://creativecommons.org/licenses/by-nc-nd/4.0/.

breast cancer [3–6]. Moreover, high ROR1 expression is closely associated with poor prognosis of cancer patients [4–6]. Increasing evidence demonstrates that ROR1 signaling is crucial for promoting tumor growth and metastasis through activating multiple pathways, including PI3K-AKT pathway [7–9]. Importantly, targeting ROR1 by short-hairpin RNAs was demonstrated to effectively repress tumor growth in vivo [10, 11]. Therefore, ROR1 is considered as an ideal target for cancer therapy.

Currently, several strategies have been developed to target ROR1, such as small molecule inhibitor [12, 13], monoclonal antibody (mAb) [14, 15], antibody-drug conjugate (ADC) [16], and chimeric antigen receptor T (CAR-T) cell therapy [17, 18]. The preclinical studies showed that these approaches are promising for hematological and solid malignancies with high ROR1 expression. The antibody-based therapy becomes a popular choice because of its high specificity and low adverse effects. For example, Zilovertamab (also called UC-961), a humanized anti-ROR1 IgG1 mAb, can block ROR1 signaling and inhibit engraftment of transgenic mouse leukemia B cells expressing human ROR1 [19]. Intriguingly, Zilovertamab exhibits long plasma half-life without discernable dose-limiting toxicity in a phase 1 study [20]. Therefore, it is urgent needs to develop novel humanized anti-ROR1 antibodies for cancer therapy.

In this study, we first confirmed the upregulated ROR1 expression in tumor tissues and cancer cells, and also validated that ROR1 has the potential as a therapeutic target. Then we successfully developed humanized anti-ROR1 antibodies, designated as h1B8 and h6D4, with high specificity and affinity. Moreover, in vitro functional experiments showed that these antibodies effectively inhibited growth and migration of cancer cells with high ROR1 expression. Notably, preclinical studies in mice demonstrated that both h1B8 and h6D4 exhibited strong anti-tumor efficacy in ROR1-positive lung cancer xenograft model, c-Myc/Alb-cre liver cancer transgenic mouse model, and MMTV-PyMT breast cancer mouse model. Therefore, this study provides novel humanized anti-ROR1 antibodies for cancer treatment.

Materials and methods

Cell lines

Human lung cancer cells (A549, H1975 and PC-9) and human breast cancer cells (MDA-MB-231 and MDA-MB-468) were maintained in RPMI-1640 (Gibco, USA) containing 10% (v/v) fetal bovine serum (FBS), 100 IU/mL penicillin and 100 μg/mL streptomycin (Biosharp, China). Human hepatocellular carcinoma cells (HCC-LM3, Huh7 and SNU398) and human embryonic kidney cell HEK293 were cultured in DMEM (Gibco, USA) supplemented with 10% FBS, 100 IU/mL penicillin and 100 μg/mL streptomycin. The 293 F cell line (Life Technologies, USA) was incubated in 293 FreeStyle serum-free medium (Life Technologies, USA) for antibody expression. All cells were cultured at 37 °C in 5% CO_2 incubator. High Five and Sf9 insect cells were maintained at 27 °C in SIM HF medium and SIM SF medium (Sino Biological, China), respectively.

For lentivirus production, pLKO.1-derived plasmid for ROR1 knockdown, packaging plasmids psPAX2 and pMD2G were co-transfected into 293T cells. Supernatants were collected at 48 h and 72 h post transfection to infect cancer cells. After 2 μg/mL of puromycin selection, stable ROR1-silenced A549, MDA-MB-231 and HCC-LM3 cells were constructed.

MTT assay and colony formation assay

For cell proliferation assay, cells were seeded into 96-well plates at a density of 1500 cells per well. At different time points, 10 μL of MTT solution (5 mg/mL) was added to each well and the plates were incubated for 3 h. After removing media, 100 μL of dimethyl sulfoxide (DMSO) was added to dissolve the formazan crystals, and the absorbance at 570 nm was measured by a microplate reader. To examine the effects of antibody on cell viability, cells were seeded into 96-well plates and then treated with varying concentrations of anti-ROR1 antibodies on the 2nd day. Cell viability was measured by MTT assay after 72 h of treatment and calculated as the following formula: viability (%) = $(OD_{treat} - OD_{blank})/(OD_{control} - OD_{blank}) \times 100\%$.

For colony formation assay, 1500 cells were seeded into 6-well plates and cultured for 14 days. During cell culture, media were replaced every three days. Finally, colonies were fixed with 4% polyformaldehyde, stained with 0.1% crystal violet (Beyotime, China) and photographed.

Transwell migration assay

For Transwell migration assay, cells were seeded in the upper layer of Transwell chamber (8 μm, Corning, USA) with 200 μL of serum-free medium, while the lower layer contained media with 10% FBS to induce cell migration. To examine the effects of antibody on cell migration, humanized anti-ROR1 antibodies (100 μg/mL) were added to the top chamber when seeding cells. After incubating for 24 h, non-migrated cells inside of Transwell were removed using a cotton swab. Then cells on the filters were fixed with 4% polyformaldehyde for 20 min and stained with 0.1% crystal violet (Beyotime, China) for another 20 min at room temperature. Pictures were acquired with a Leica DMi8 microscope.

Wound healing assay

Cell monolayer was scraped by a 200 μL pipette tip and washed with PBS twice when cells reached up to 95% confluence in a 6-well plate. Then cells were cultured in

medium containing 1% FBS and 1% penicillin/streptomycin. Images were captured at 0, 24, 48, and 72 h following the initial scratch of each wound. Image J software (NIH, USA) was used to calculate the cell wound healing rate as follows: (the original wound areas - the actual wound areas at different times)/ (the original wound areas).

Flow cytometry

To assess ROR1 expression, both cancer cell lines and primary cells derived from mouse tumor tissues were subjected to flow cytometry. Tumor tissues from mice were minced and dissociated into single-cell suspensions using a collagenase/pancreatin solution and the GentleMACS Octo Dissociator with Heaters (Miltenyi Biotec, Germany). The single-cell suspensions were then prepared to a density of 10^7 cells/mL in PBS, and 100 µL of cell suspensions were incubated on ice for 30 min with APC anti-ROR1 antibody (Biolegend, USA) or APC Isotype control antibody (Biolegend, USA). After washing three times with wash buffer, cells were collected into FACs tubes to perform flow cytometry.

To evaluate the binding ability of humanized anti-ROR1 antibodies, cells were incubated with h1B8 antibody, h6D4 antibody, or the isotype control antibody, followed by incubation with FITC-conjugated goat anti-human IgG secondary antibody (Invitrogen, USA). FACS analyses were conducted using an LSR Fortessa (BD, USA) or CytoFLEX (Beckman Coulter, USA) flow cytometer.

Antibody internalization assay

Cells were incubated with 1 µg/mL of humanized anti-ROR1 antibody or the isotype control antibody at 4 °C for 30 min, followed by washing with pre-chilled PBS containing 2% FBS. Then the internalization group was incubated at 37 °C for indicated times, while the control group remained at 4 °C. At each time point, cells were transferred to 4 °C and labeled with FITC-conjugated anti-human IgG antibody (diluted at 1:1000) for 30 min on ice. Finally, cells were washed three times with cold PBS and suspended in PBS for flow cytometric analysis.

Preparation of recombinant proteins

The DNA fragment encoding ROR1-ECD (extracellular domain) was cloned into the pFastBac™ HT vector (Invitrogen, USA) at *Bam*HI and *Xho*I sites. The resultant plasmids were transfected into Sf9 insect cells to prepare baculovirus following the user manual of the Bac-to-Bac Baculovirus Expression System. After three rounds of virus amplification, High Five cells were infected with the baculovirus to express the N-terminal His-tagged ROR1-ECD for 60 h, followed by filtration through a 0.45 µm filter to collect supernatants. Then the recombinant proteins were purified by the Ni-NTA affinity agarose resin (Cytiva, USA) with elution buffer (20 mM Tris-HCl, 150 mM NaCl, 300 mM imidazole, pH 8.0) and further purified by a Q-ion-exchange column (Cytiva, USA).

Construction of humanized antibody-expressing vectors

The 1B8 and 6D4 murine antibodies were generated using the standard hybridoma technology. The mouse hybridoma cells were used to clone variable domains of anti-ROR1 antibody by the FirstChoice™ RLM-RACE Kit (Invitrogen, USA) according to the manufacturer's instructions. The primers were listed in table S1. 5'RACE products (VH and VL) were cloned into the pMD19-T vector (TaKaRa, China) and sequenced. Subsequently, IMGT (https://www.imgt.org/) was used as the reference database and IgBlast (https://www.ncbi.nlm.nih.gov/igblast/) was utilized to identify the framework region (FR) and complementarity-determining regions (CDR) according to Kabat/IMGT numbering system. Next, the humanization of murine mAb was achieved by CDR grafting. The CDRs were grafted into the most appropriate human VH/VL frameworks and paired with human Fc domains from IgG1 to assemble the complete humanized antibody. To maintain the optimal CDR loop structure, computer-aided design was employed to simulate the spatial conformation of antibodies and identify critical amino acids for residue mutation analysis. In summary, the combination of 4 VH chains and 3 VL chains for the antibody 1B8 resulted in 12 humanized antibody variants, while the combination of 3 VH chains and 4 VL chains for the antibody 6D4 generated 12 humanized antibody variants.

Expression and purification of humanized antibodies

The nucleotide sequences of heavy chain and light chain of anti-ROR1 antibodies, after codon optimization, were synthesized and cloned into the pcDNA3.1(+) vector by GENEWIZ Inc. (China). HEK293F cells were co-transfected with heavy and light chain plasmids by polyethyleneimine (PEI) to express recombinant antibodies and cultured for 7 days. The cell culture supernatants were collected to purify antibodies by MabSelect™ PrismA column, followed by Size Exclusion Chromatography with Superdex® 200 Increase 10/300 GL column by the AKTA FPLC System (Cytiva, USA). Then the eluted antibodies were concentrated using Amicon Ultra-15 centrifugal filters (Millipore, USA), followed by buffer exchange into 1× PBS. Finally, antibody solutions were filtered by 0.22 µm sterile filters before being divided into aliquots for storage.

Surface plasmon resonance (SPR)

The interaction between antibody and antigen was monitored using SPR spectroscopy with Biacore X100 instrument (Cytiva, USA). Briefly, the purified His-tagged

extracellular domain of ROR1 was immobilized on the carboxy-methylated dextran sensor chip (Sensor Chip CM5). The final levels of immobilization were approximately 550 response units. Nine concentrations of each humanized antibody variant were added to the buffer flowing over the chip in the multiple cycle kinetics (250, 125, 62.5, 31.25, 15.63, 7.81, 3.91, 1.95, 0.97 nM, flow rate: 30 μL/min, contact time: 120 s, dissociation time: 300 s). Binding experiments were performed at 25 °C in a running buffer containing 10 mM HEPES pH 7.2, 150 mM NaCl, and 0.05% Tween-20. Dissociation equilibrium constant (K_D) values were calculated by affinity fitting using the Biacore X100 evaluation software (Cytiva, USA).

ELISA assay

The recombinant ROR1-ECD protein was diluted to 1 μg/mL and used for coating the 96-well ELISA plate overnight at 4 °C. Then the plate was washed three times with PBST, followed by blocking with 200 μL of 5% skim milk at 37 °C for 1 h and subsequent incubation with tested antibody solution at 37 °C for 1 h. After extensive washing, the plate was incubated at 37 °C with HRP-conjugated goat anti-human or goat anti-mouse secondary antibody for 1 h. Then, 100 μL of substrate solution was added into each well and the plate was incubated in the dark at room temperature for 10 min, followed by adding 100 μL of 2M H_2SO_4 into each well to stop reactions. Finally, the absorbances at 450 nm were measured by a microplate reader.

Immunoblotting

Cells were treated with antibodies (100 μg/mL) for 24 h and then lysed by the RIPA buffer (Beyotime, China) containing a cocktail of protease and phosphatase inhibitors (Beyotime, China). After determining protein concentrations using BCA assays, equal amounts of proteins were loaded onto SDS-PAGE gels along with a protein marker (cat#26616, Thermo, USA) and then transferred onto PVDF membranes (Millipore, USA). The membranes were blocked with 5% BSA at room temperature for 1 h and incubated overnight at 4 °C with antibodies against p-AKT (cat#9271, CST, USA), AKT (cat#9272, CST, USA), or GAPDH (cat#3683, CST, USA). Then membranes were washed three times with TBST, incubated with secondary antibodies conjugated with horseradish peroxidase for 1 h. After extensive washing with TBST three times, signals were detected using an enhanced chemiluminescence detection kit (Thermo, USA).

Animal studies

Balb/c nude mice (4 weeks, female) were purchased from HuaFukang Biological Technology Co., Ltd. (China). H11-CAG-LSL-Myc mice (C57BL/6J background) were purchased from Shanghai Model Organisms Center, Inc. (China). The MMTV-PyMT transgenic mice (FVB background) were purchased from GemPharmatech Co., Ltd. (China). All mice were maintained on a 12-hour light/12-hour dark cycle at 25 °C under specific pathogen-free conditions.

Subcutaneous tumor model of lung cancer

H1299-ROR1 cells (5×10^6) and A549 cells (6×10^6) were respectively mixed with Matrigel (BD Biosciences, USA) at a 1:1 ratio in a total volume of 100 μL and injected subcutaneously into the flanks of nude mice. When the average tumor volume reached 50 mm^3, mice were randomly assigned to control and treatment groups. Anti-ROR1 antibodies (5 mg/kg) were administered via intraperitoneal injection twice weekly for 3 weeks. The tumor volumes and body weights were measured until the end of experiments. Tumor volumes were calculated using the formula: V (volume) = (length × $width^2$)/2. At the end of experiments, tumor tissues were collected, weighed and photographed. The heart, liver, spleen, lung and kidney of mice were collected for Hematoxylin and Eosin (H&E) staining. The blood supernatant was obtained by centrifugation after blood was collected from mouse's orbit, and stored at −80 °C.

$H11^{LNL-myc}$ knock-in HCC mouse model

C-Myc/Alb-cre double-positive ($Myc^{KI/KI}$) C57BL/6J mice were generated by crossing $H11^{LNL-Myc}$ heterozygous mice with Alb-cre transgenic mice. Mice were identified by PCR genotyping at 4 weeks of age. C-Myc/Alb-cre transgenic mice were randomly divided into three groups (control, h1B8-mIgG2a, h6D4-mIgG2a) with 6 mice in each group. Mice were treated with different humanized anti-ROR1 antibodies (5 mg/kg, 100 μL) via tail-vein injections twice a week for a total of six injections. Finally, mice were euthanized and their livers were harvested, photographed, and fixed with 4% paraformaldehyde for histopathological examination. Meanwhile, other main organs of the mice were collected for H&E staining. The blood supernatant was obtained by centrifugation after blood was collected from mouse orbit, and stored at −80 °C.

MMTV-PyMT breast cancer model

Female MMTV-PyMT mice developed mammary tumors spontaneously. The genotype of the mice was identified by PCR at 4 weeks after birth, and the amplification of MMTV-PyMT mice resulted in 556 bp PCR products. Breast cancer transgenic mice were randomly divided into three groups: control, h1B8-mIgG2a, and h6D4-mIgG2a (6 mice per group). Mice were intraperitoneally injected at a dosing of 5 mg/kg of antibody, twice a week for a total of six injections. The weight of each

mouse was monitored. At the end point, mice were sacrificed and their blood and organs (heart, liver, spleen, lung, and kidney) were collected and prepared for subsequent experiments.

Histopathology and immunohistochemistry assay

Upon fixation in 4% paraformaldehyde for 24 h, dehydration using an automatic dehydrator for 16 h, and embedding in a paraffin embedding machine, mouse tissue sections were prepared. The paraffin sections. (4 μm) were dewaxed using xylene and rehydrated using a gradient of alcohol. For histopathological analysis, after dewaxing and rehydrating tissue sections, they were stained with hematoxylin staining solution for 10 min, followed by rinsing with water. Subsequently, a 0.5% hydrochloric acid ethanol solution was used for differentiation to distinguish cell structures, and then the sections were treated with eosin staining solution for 10 s. After staining, the sections were air-dried and mounted with neutral resin. Finally, the mounted sections were scanned using a pathological section scanning machine to obtain digital image data for further analysis. The analysis of the results was conducted with the Inform software (Akoya Biosciences, USA). The impact of antibody treatment was assessed by randomly selecting three high-power fields and evaluating the percentage of tumor tissue within these fields.

For immunohistochemistry analysis, the tissue microarray slides for human lung cancer (cat# HLugA030PG04), breast cancer (cat# HBreD030CS01), and liver cancer (cat# OD-CT-DgLiv01-011) were purchased from Shanghai Outdo Biotech Company (China) for ROR1 immunostaining. The antigens were retrieved using a sodium citrate buffer (20 mM, pH 6) at 80 °C for 15 min. Tissue sections were allowed to cool to room temperature and then washed for three times in PBS. Then, 3% H_2O_2 was applied for 15 min to block endogenous peroxidase activity, followed by blocking non-specific binding sites with 5% goat serum for 45 min. Afterwards, the sections were incubated overnight at 4 °C with anti-ROR1 antibody (diluted at 1:200). Following three additional washes in PBS, the sections were incubated with HRP-conjugated secondary antibodies at room temperature for 45 min. Further washing with PBS was carried out for three times. The color reaction was developed using DAB chromogen (CST, USA), and the sections were subsequently counterstained with hematoxylin. Finally, the sections were dehydrated and mounted. The results were analyzed using the Inform software (Akoya Biosciences, USA).

Statistical analysis

Statistical analyses were performed using GraphPad Prism 8.0 (GraphPad Software Inc., USA). The statistical differences between groups were assessed using Student's *t*-test for two-group comparisons or two-way analysis of variance (ANOVA) for multiple comparisons. Probability values (p) less than 0.05 were considered statistically significant ($^{*}p<0.05$, $^{**}p<0.01$, $^{***}p<0.001$, $^{****}p<0.0001$); P values greater than 0.05 were considered not significant (ns).

Results

Targeting ROR1 effectively inhibits the proliferation and migration of cancer cells

Previous studies suggested that ROR1 is upregulated in tumor tissues and plays an important role in tumor progression [3, 21], prompting us to explore the potential of ROR1 as a therapeutic target. Firstly, we performed immunohistochemistry staining to analyze ROR1 expression using lung cancer, breast cancer and liver cancer tissue microarrays, and the results indicated significantly higher expression of ROR1 protein in tumor tissues, correlating positively with metastasis in breast cancer (Fig. 1A). Furthermore, ROR1 was found to be extensively overexpressed in breast cancer cells (MDA-MB-231 and MDA-MB-468), lung cancer cells (A549, H1975 and PC-9) and liver cancer cells (LM3, Huh7 and SNU398), as determined by flow cytometric analyses (Fig. 1B). To examine the functions of ROR1 in cancer cells, two shRNAs were designed to generate stable cell lines. The results showed that ROR1 expression was successfully knocked down by shRNAs in LM3, A549 and MDA-MB-231 cells (Fig. 1C). Colony formation assays (Fig. 1D) and MTT assays (Fig. S1A) indicated that ROR1 depletion effectively inhibited cell proliferation. Transwell migration assays (Fig. 1E) and wound-healing experiments (Fig. S1B) demonstrated that ROR1 knockdown significantly decreased the migratory ability of tumor cells. Based on these observations, we conclude that targeting ROR1 can effectively inhibit the proliferation and migration of cancer cells, implying that ROR1 is a potential target for cancer therapy.

Murine monoclonal anti-ROR1 antibodies suppress tumor growth

We utilized the hybridoma technology to generate ROR1-specific monoclonal antibodies (mAbs) from mice that were immunized with H1299 cells stably overexpressing ROR1 (Fig. S2A). As a result, we obtained four positive hybridoma cell lines. Purified mAbs from these hybridomas were then evaluated for their specificity to ROR1 using flow cytometric analysis and ELISA assays. Flow cytometric analyses revealed that mAbs 1B8, 3E5, and 6D4 exhibited high binding activity to ROR1 expressed on the cell membrane, whereas 2F1 had low binding activity (Fig. 2A). Using a Bac-to-Bac expression system, we expressed the extracellular domain of ROR1 (ROR1-ECD) with a N-terminal 6×His tag in insect cells

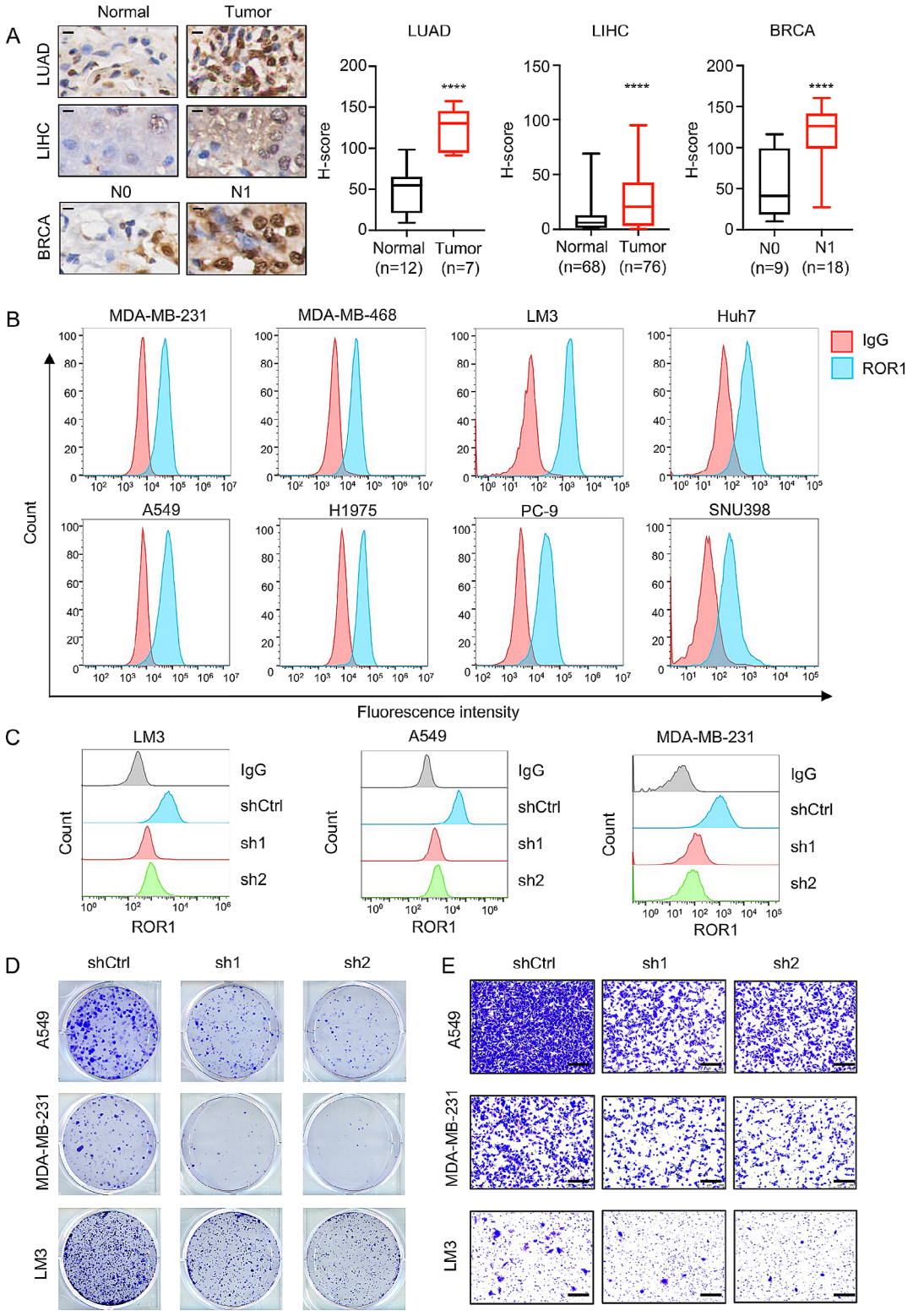

Fig. 1 Targeting ROR1 effectively inhibits the proliferation and migration of cancer cells. **(A)** Representative immunohistochemistry images and H-score of ROR1 expression from tissue microarrays of lung, liver, and breast cancer samples. N0: no regional lymph nodes metastasis; N1: regional lymph nodes metastasis. H-score was quantified by inForm software. Scale bar, 50 μm. **(B-C)** Flow cytometric analysis of ROR1 expression in lung, liver, and breast cancer cells **(B)**, as well as in ROR1-knockdown tumor cells **(C)**. **(D-E)** Effects of ROR1 knockdown on colony formation **(D)** and migration **(E)** of LM3, A549 and MDA-MB-231 cells. Scale bar, 250 μm

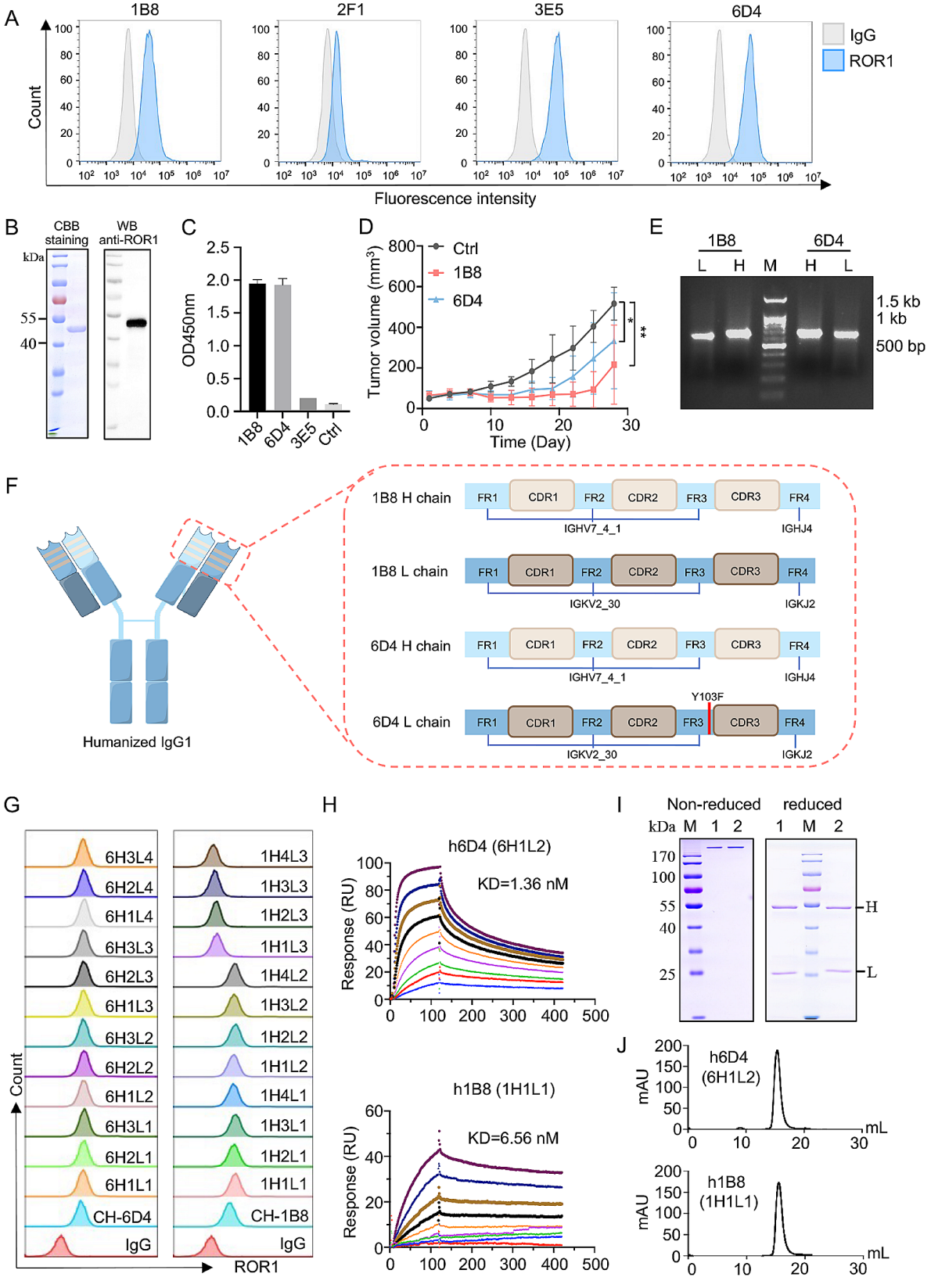

Fig. 2 (See legend on next page.)

(See figure on previous page.)

Fig. 2 Development and characterization of humanized anti-ROR1 antibody. **(A)** Flow cytometry was used to detect the binding ability of murine anti-ROR1 mAbs (purified from hybridoma supernatants) to ROR1 protein on the surface of MDA-MB-231 cells. **(B)** Coomassie brilliant blue staining (left) and immunoblotting (right) of purified recombinant extracellular domain of ROR1 protein. **(C)** ELISA assays show the binding of murine anti-ROR1 antibodies to recombinant extracellular domain of ROR1 protein. **(D)** Tumor growth curves of H1299-ROR1 xenograft in mice treated with control, 1B8, and 6D4 antibodies. **(E)** Agarose gel analysis of 5′RACE products from 1B8 and 6D4 hybridoma. H, heavy chain; L, light chain. **(F)** Schematic representation of humanized anti-ROR1 antibodies. CDR sequences of 1B8 and 6D4 were defined and inserted into the FR sequence of selected human IgG1. The light chain of 6D4 contains a revertant mutation (marked by red color). **(G)** Flow cytometric analyses show the binding of 24 humanized antibody variants to ROR1 proteins on cell surface. **(H)** SPR analyses of h1B8 and h6D4 antibodies. **(I)** The purity of h1B8 and h6D4 antibodies were examined by SDS-PAGE under non-reduced (left) and reduced (right) conditions followed by Coomassie brilliant blue staining. Label 1 represents h1B8; label 2 represents h6D4. **(J)** Size exclusion chromatograms of purified h1B8 and h6D4 antibodies

and purified the fused protein (Fig. 2B), which was then subjected to ELISA assays. The results indicated that 1B8 and 6D4 mAbs were capable of recognizing the recombinant ROR1-ECD protein (Fig. 2C). To further characterize which part of the extracellular domain of ROR1 protein binds to 1B8 and 6D4 antibodies, we expressed and purified five Fc-fused proteins, each containing one or two extracellular domains of human ROR1 protein. Then these proteins were subjected to ELISA assays. The results showed that both 1B8 and 6D4 antibodies recognized Fc-hROR1-Ig+Fz, but didn't bind to the immunoglobulin-like domain (Ig) or the Frizzled domain (Fz) (Fig. S2B), implying that the epitopes of these mAbs are likely in the region between Ig and Fz domains or specific conformation formed by both domains. Finally, we evaluated the anti-tumor activity of 1B8 and 6D4 antibodies in the subcutaneous xenograft mouse model and found that both antibodies effectively suppressed tumor growth (Fig. 2D).

Humanization of 1B8 and 6D4 antibodies

Due to the impressive in vivo anti-tumor efficacy of the murine monoclonal antibodies 1B8 and 6D4, we decided to develop their humanized versions for future clinical applications. The humanization of murine anti-ROR1 antibodies was achieved through the CDR grafting technique [22]. Initially, ELISA analysis identified the murine anti-ROR1 antibodies (1B8 and 6D4) as IgG1 Fc subtype with a kappa (κ) light chain (Fig. S2C). Then, we designed specific primers for 5′RACE and RT-PCR to amplify the variable regions of 1B8 and 6D4 (Fig. 2E and Fig. S2D). Subsequently, the specified murine CDRs were integrated into the framework regions (FRs) of human IgG sequence, which was selected from germline genes based on its homology with ROR1 (Fig. 2F). DNA sequences encoding the amino acid sequence of humanized variants were synthesized and cloned into the pcDNA 3.1(+) expression vector. Twelve humanized variants were derived from the parental murine antibody 1B8, and twelve variants were created from the murine antibody 6D4. These variants consist of murine-derived CDRs and humanized heavy and light FRs.

Characterization of humanized anti-ROR1 antibodies

It is very important to maintain the antibody's specificity and affinity for its target during antibody humanization. We screened all humanized antibody variants of 1B8 and 6D4 (cell supernatants) for their specific binding and affinity towards human ROR1 antigen using flow cytometry (Fig. 2G) and ELISA (Fig. S2E). The results showed that all humanized 6D4 variants maintained similar or improved specificity and efficient binding compared to their parental antibody. However, four humanized 1B8 antibody variants (1H1L3, 1H2L3, 1H3L3, 1H4L3) did not exhibit this property. Moreover, SPR assays were performed to further confirm the binding affinity between recombinant ROR1-ECD protein and purified antibody variants (Fig. S2F). As shown in Table 1, each variant of both 1B8 and 6D4 antibodies demonstrates low nanomolar range (10^{-8}-10^{-9} M) of equilibrium dissociation constant (K_D) values, typically indicative of high-affinity antibodies. Among humanized 1B8 variants, 1H1L1 exhibited the highest affinity for recombinant ROR1-ECD protein, while the one with the strongest affinity was 6H1L2 among humanized 6D4 variants (Fig. 2H). Thus, we selected these two humanized antibody variants, which are hereafter called as h1B8 and h6D4, respectively, for further investigations.

To examine biological activities of humanized anti-ROR1 mAbs, we expressed h1B8 and h6D4 antibodies in a large scale using the HEK293F system and purified them by Protein A affinity chromatography and size exclusion chromatography. The purified antibodies were detected by SDS-PAGE electrophoresis. Under non-reducing conditions, a single band at ~170 kDa was clearly observed. Under reducing conditions, the target bands at approximately 50 kDa (heavy chain) and 25 kDa (light chain) appeared, indicating that two humanized antibodies were expressed correctly and assembled completely (Fig. 2I). Moreover, the purified humanized mAbs had high purities (>95%), as verified by size exclusion chromatography (Fig. 2J).

The specificity and anti-tumor potential of humanized h1B8 and h6D4 antibodies

To further confirm the specific binding and affinity of humanized antibodies h1B8 and h6D4 toward native

Table 1 SPR data of humanized 1B8 and 6D4 antibodies

Humanized 6D4	SPR-K_D (M)	Humanized 1B8	SPR-K_D (M)
6H1L1	3.74E-09	**1H1L1**	**6.56E-09**
6H2L1	2.17E-09	1H2L1	1.34E-08
6H3L1	2.58E-09	1H3L1	2.31E-08
6H1L2	**1.36E-09**	1H4L1	1.05E-08
6H2L2	6.24E-09	1H1L2	2.33E-08
6H3L2	5.61E-09	1H2L2	2.00E-08
6H1L3	3.08E-09	1H3L2	1.61E-08
6H2L3	3.41E-09	1H4L2	1.38E-08
6H3L3	3.52E-09	*CH-1B8	1.53E-08
6H1L4	3.43E-09		
6H2L4	2.22E-09		
6H3L4	2.28E-09		
*CH-6D4	1.87E-08		

* Chimeric 1B8 and 6D4, which possess the murine variable domains and the human IgG1 constant domains, were used as reference samples

ROR1 protein on cell surface, flow cytometric analyses were performed using different cancer cells with or without ROR1 expression. The results showed that both antibodies exhibited specific binding to ROR1 on the surface of cancer cells, with h6D4 showing a greater affinity than h1B8 (Fig. 3A). The efficacy of monoclonal antibodies for cancer therapy depends on their capacity to target cancer cells, and in certain cases, receptor-mediated internalization of antibody into cells is also necessary [23]. Thus, we compared the internalization of humanized anti-ROR1 antibodies by flow cytometry, and the results showed that the h1B8 antibody displays a greater capacity for internalization compared to h6D4, with maximum internalization occurring at 30 min and nearly complete internalization at 4 h (Fig. 3B).

The biological activities of these two antibodies were evaluated in cancer cells. In MTT assays, both h1B8 and h6D4 antibodies inhibited the proliferation of A549, MDA-MB-231 and LM3 cells (with high ROR1 expression) in a concentration-dependent manner, but have little effects on H1299 cells (without ROR1 expression) (Fig. 3C), demonstrating that both antibodies specifically target ROR1 to repress cell proliferation. Similarly, colony formation assays showed that treatment with both anti-ROR1 antibodies significantly reduced clone numbers (Fig. 3D). Moreover, Transwell migration assays indicated that both humanized antibodies effectively inhibited tumor cell migration when ROR1 was highly expressed (Fig. 3E).

The antibody-dependent cell-mediated cytotoxicity (ADCC) relies on cell-mediated immunity, where the effector cells actively lyse tumor cells which have been bound by a specific antibody. To determine the ADCC potential of our humanized antibodies, we evaluated their efficacy to kill MDA-MB-231 cells by ADCC using lactate dehydrogenase (LDH) release assays. As shown in Fig. S3, both h1B8 and h6D4 antibodies can medicate cytotoxic killing of target cancer cells in a dose-dependent manner when assayed with isolated human peripheral blood mononuclear cells (PBMCs) from healthy donors. ROR1 was reported to activate AKT signaling, so we examined the effects of humanized anti-ROR1 antibodies on AKT phosphorylation status. The results showed that both antibodies indeed decreased phosphorylation of AKT (p-AKT), but have little effects on AKT protein levels in A549, MDA-MB-231 and LM3 cells with high ROR1 expression (Fig. 3F). Moreover, such effects were not observed in H1299 cells without ROR1 expression (Fig. 3F). Therefore, humanized h1B8 and h6D4 antibodies effectively suppressed tumor cell proliferation and migration in a ROR1-dependent manner.

Humanized h1B8 and h6D4 antibodies suppress tumor growth in lung cancer xenograft mice

The in vivo effects of humanized anti-ROR1 antibodies on tumor growth were investigated using the A549 subcutaneous xenograft tumor mouse model (Fig. 4A). The results showed that treatment of tumor-bearing mice with either anti-ROR1 antibodies significantly reduced tumor growth (Fig. 4B-D), has little effect on mouse body weight (Fig. 4E). Acccordingly, the tumor weight-to-body weight ratios dramatically decreased after treatment with both antibodies (Fig. 4F). Moreover, H&E staining showed that administration of both antibodies did not induce the damage of organs, such as heart, liver, spleen, lung and kidney (Fig. 4G). In addition, no significant differences were detected in blood biochemical indexes (ALB, ALP, and ALT) of antibody treatment groups compared with control group (Fig. 4H), indicating negligible hepatotoxicity.

Humanized h1B8 and h6D4 antibodies alleviate HCC progression in transgenic mice

The c-Myc/Alb-cre double-positive mice were reported to develop HCC tumors [24], so we employed this transgenic mouse model to examine the effects of humanized anti-ROR1 antibodies on tumor progression. First, we identified high expression of ROR1 in liver tumors of mice by flow cytometry (Fig. 5A) and immunohistochemistry (Fig. 5B). Then humanized anti-ROR1 antibodies were administrated twice a week via tail-vein injection (Fig. 5C). As expected, humanized h1B8 and h6D4 antibodies dramatically reduced liver cancer in the transgenic mice, as indicated by a significant decrease in tumor areas on H&E staining compared to the control mice. Notably, the h1B8 antibody exhibited a more pronounced therapeutic effect than h6D4 (Fig. 5D, E). Administration of antibodies did not affect body weight (Fig. 5F), and no obvious toxicity to heart, spleen, lung and kidney of mice was observed (Fig. 5G). Importantly, antibody treatment effectively alleviated the elevation of

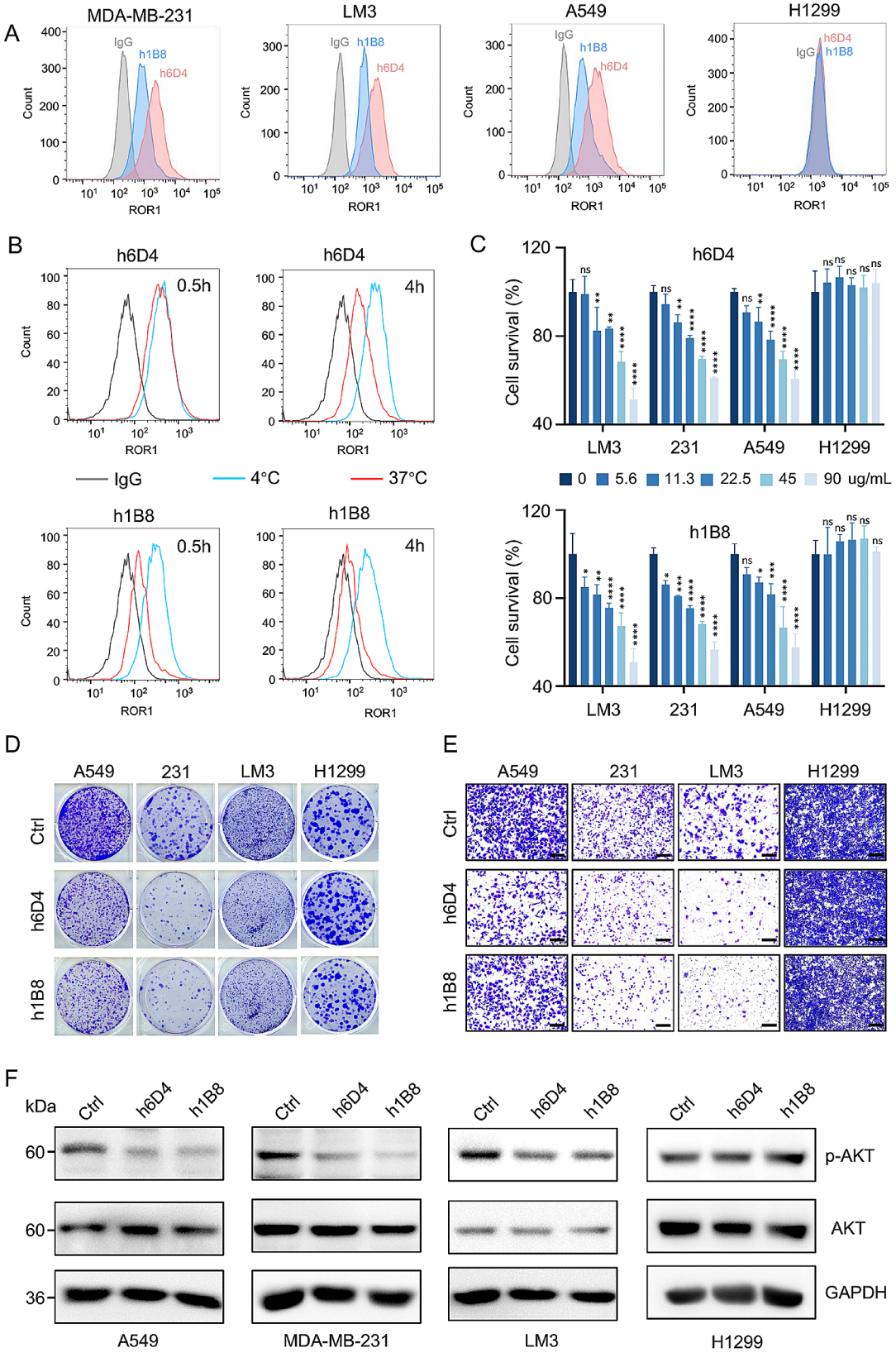

Fig. 3 (See legend on next page.)

(See figure on previous page.)

Fig. 3 In vitro characterization of humanized h1B8 and h6D4 antibodies. **(A)** Flow cytometric analyses show the binding ability of h1B8 and h6D4 antibodies to ROR1$^+$ or ROR1$^-$ cells. **(B)** Internalization analyses of h1B8 and h6D4 antibodies into cancer cells. Cells were incubated with antibodies at 4 ℃ to inhibit internalization or at 37 ℃ to induce internalization before flow cytometric analysis. **(C)** Effects of h1B8 and h6D4 antibodies on cell viability. Cells were cultured with different concentrations of anti-ROR1 antibodies for 72 h, and then subjected to MTT assays. **(D)** Effects of h1B8 and h6D4 antibodies on cell growth. Cancer cells was treated with 100 μg/mL of antibodies for certain times and then subjected to colony formation assays. **(E)** Representative images of Transwell migration assays in cells with or without incubation of h1B8 and h6D4 antibodies (100 μg/mL). **(F)** Immunoblotting analyses show the effects of h1B8 and h6D4 antibodies on AKT signaling in different cancer cells upon anti-ROR1 antibody treatment (100 μg/mL)

alanine aminotransferase ALT) and ALP levels caused by liver cancer, as evidenced by blood biochemical tests (Fig. 5H).

Humanized h1B8 and h6D4 antibodies inhibit lung metastasis in the MMTV-PyMT breast cancer model

Previous studies show that breast tumors exhibit high expression of ROR1 proteins [11, 14]. To further confirm anti-tumor effect of humanized h1B8 and h6D4 antibodies, we employed the MMTV-PyMT breast cancer mouse model. First, we validated high expression of ROR1 in breast tumors by flow cytometry (Fig. 6A) and immunohistochemistry (Fig. 6B). In the MMTV-PyMT breast cancer mouse model, lung is the common site of metastasis. Thus, we treated mice with antibodies by intraperitoneal injection twice a week (Fig. 6C) and then observed pulmonary metastasis. The results showed that humanized h1B8 and h6D4 antibodies dramatically inhibited lung metastasis (Fig. 6D, E), but have no noticeable effects on body weight (Fig. 6F). Remarkably, the splenomegaly induced in the mice with breast cancer was alleviated by both antibodies (Fig. 6G, H). H&E staining of major organs and blood biochemical indexes showed no obvious toxicity in these three groups (Fig. 6I, J). Overall, these data indicate that humanized h1B8 and h6D4 antibodies possess substantial therapeutic efficacies in vivo.

Discussion

ROR1 is recognized to possess the characteristics of tumor-associated antigens, with numerous studies reporting its association with human cancers [3, 21, 25]. This aligns with the findings described in Fig. 1 and Fig. S1, indicating that ROR1 promotes growth and migration of cancer cells and suggesting that ROR1 could be a potential target for cancer therapy. Targeted therapy for cancer, especially the treatment employing monoclonal antibodies, has shown significant potential in clinical practice [26–28]. Till now, here is only one humanized monoclonal antibody targeting ROR1, Zilovertamab, currently undergoing clinical trials for chronic lymphocytic leukemia. Our work has successfully developed novel humanized monoclonal antibodies against ROR1, named h1B8 and h6D4 (Fig. 2, and Fig. S2). In vitro biological activity data demonstrated that their ability to inhibit tumor cell proliferation and migration in a ROR1-dependent manner (Fig. 3). Moreover, both humanized anti-ROR1 antibodies exhibited promising anti-tumor effects in three different mouse models with ROR1-positive tumors (Figs. 4, 5 and 6), supporting that they are ideal candidates for targeted therapy against ROR1-positive solid tumors.

Daneshmanesh et al. immunized mice with different domain of the extracellular part of ROR1 protein to generate murine monoclonal antibodies against ROR1 [15]. In this study, we chose H1299 stable cells that overexpress ROR1 proteins as antigens to immunize mice because of the following advantages: ROR1 was successfully expressed and located on the cell membrane surface (Fig. S2A) and also plays oncogenic roles in cell proliferation and migration [13]. Compared with traditional protein immunization strategies, whole cell immunization can benefit from higher immunogenicity, naïve antigen conformation and avoid the protein purification process, thus specifically suitable for antibody discovery against membrane protein (extracellular domain) [29]. Since application of mouse-derived monoclonal antibodies to human will trigger human anti-mouse antibody immune responses, thus reducing their effects [30], so we employed the CDR grafting technique [22] to successfully develop humanized anti-ROR1 antibodies, h1B8 and h6D4, consisting of murine-derived CDRs and humanized heavy and light FRs. During antibody humanization, we decoded the N-terminal signal peptides of both light and heavy chains, and realized their importance in directing protein synthesis and secretion [31]. Subsequently, we replaced the original signal peptides with the human IgG Kappa signal peptide, through which we successfully produced active humanized antibodies. The humanized 1H1L1 antibody exhibits the highest affinity in the 1B8 group, while the humanized 6H1L2 antibody has the highest affinity in 6D4 group (Table 1). Therefore, we chose these variants and designated them as h1B8 and h6D4 for further investigations.

With the successful application of monoclonal antibody to cancer therapy, (ADCs have emerged as powerful tools for targeted cancer therapy [32]. The effectiveness of ADCs largely depends on their ability to be internalized by tumor cells. Fast antibody internalization can improve efficiency of ADCs [33], so we evaluated the internalization capabilities of h1B8 and h6D4 antibodies and found that h1B8 exhibited stronger internalization compared to h6D4, indicating that h1B8 is more suitable for subsequent development of ADC drugs. At present, ADC drugs targeting ROR1 such as Zilovertamab Vedotin

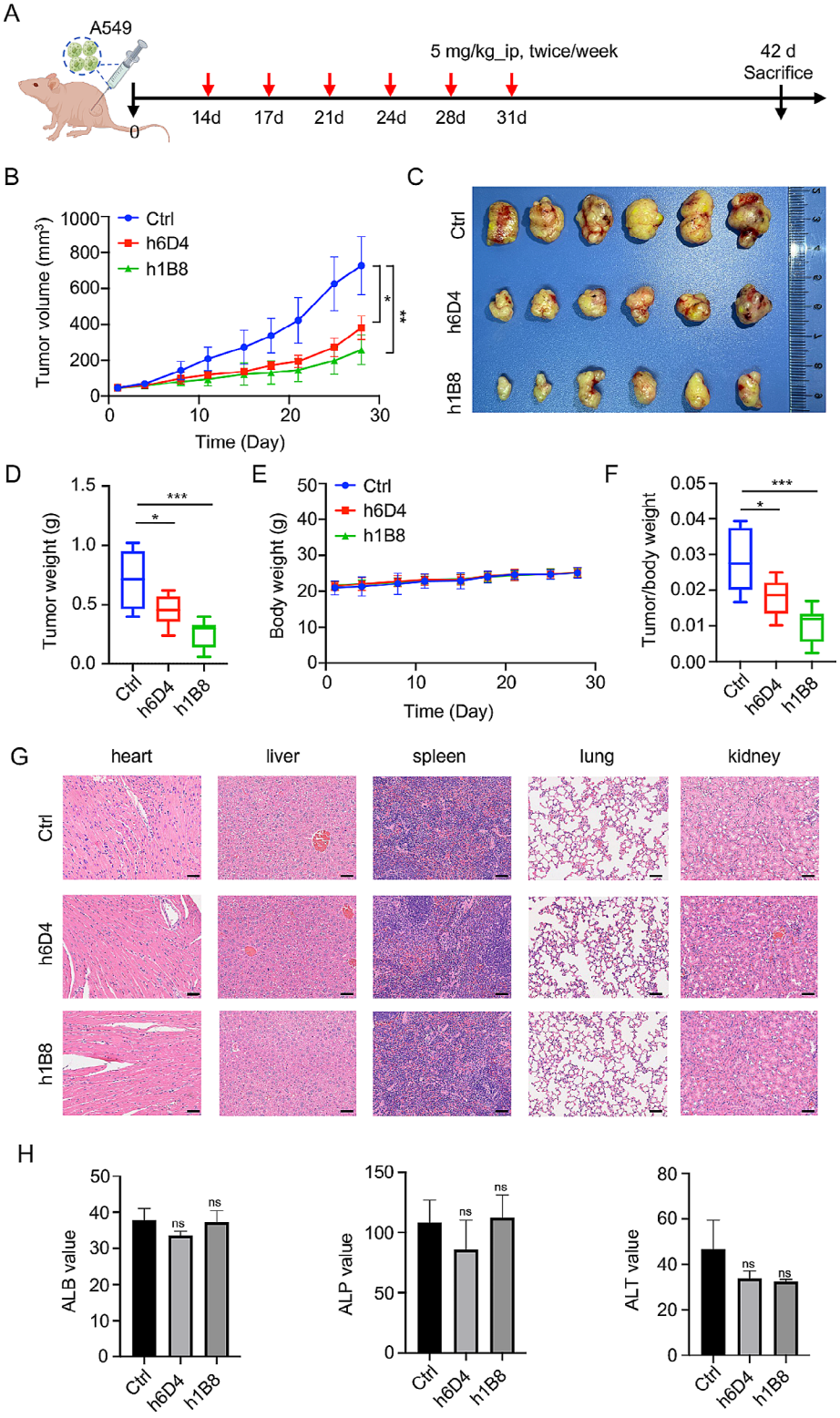

Fig. 4 Humanized h1B8 and h6D4 antibodies suppress tumor growth in lung cancer xenograft mice. **(A)** A549 cells were subcutaneously injected into nude mice to establish lung cancer xenograft model. 14 days later, mice were administrated by intraperitoneal injection of anti-ROR1 antibodies or vehicle control (5 mg/kg, twice a week, totally six times). **(B-E)** Tumor growth curves **(B)**, tumor pictures **(C)**, tumor weights **(D)**, and body weights **(E)** from A549 xenograft mice treated with or without anti-ROR1 antibodies. **(F)** The ratios of tumor weights to body weights of each group. **(G)** Representative H&E staining images of major mouse organs. Scale bar, 50 μm. **(H)** Biochemical analyses of alanine transaminase (ALT), albumin (ALB), and alkaline phosphatase (ALP) in the blood from different mice

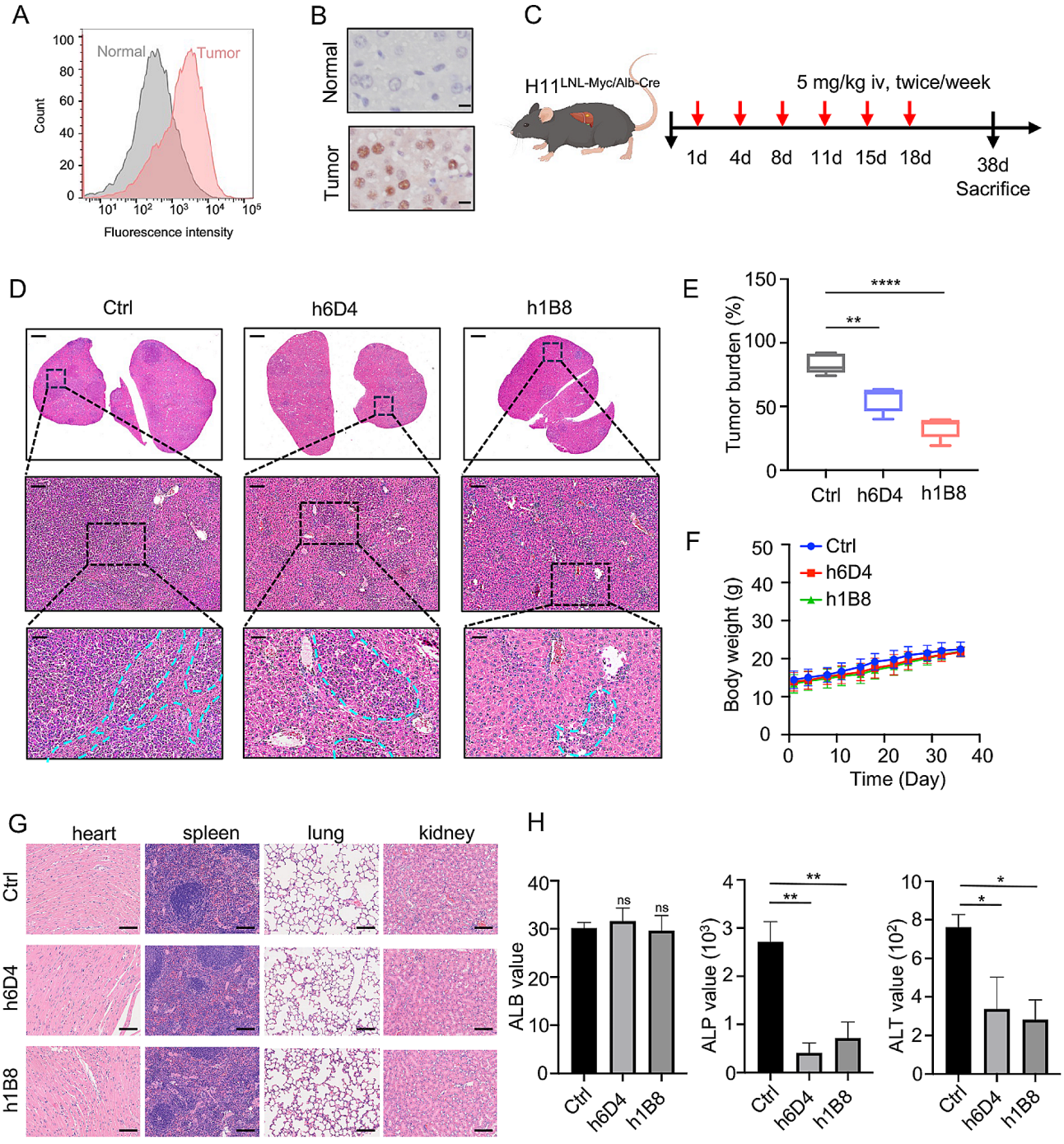

Fig. 5 Humanized h1B8 and h6D4 antibodies alleviate HCC progression in transgenic mice. **(A-B)** Flow cytometric analysis **(A)** and immunohistochemistry assays **(B)** were conducted to examine ROR1 protein expression in HCC tumor tissues. Scale bar, 50 μm. **(C)** Schematic representation of animal experiments. Mice were administrated by anti-ROR1 antibodies (5 mg/kg) or the vehicle control via tail-vein injection (twice a week, totally six times). **(D)** Representative H&E staining images of livers from each group (tumors are indicated by the blue dashed line). Scale bar: Upper, 1 mm; Middle, 100 μm; Lower, 50 μm. **(E-F)** Tumor burden **(E)** and body weights **(F)** of mice treated with or without anti-ROR1 antibodies. **(G)** H&E staining images of major mouse organs. Scale bar, 50 μm. **(H)** Biochemical analyses of ALT, ALB, and ALP in the blood from different mice

(MK-2140) (NCT04504916, NCT03833180) and CS5001 (NCT05279300) are undergoing clinical trials. Therefore, we will develop ADCs based on our anti-ROR1 antibodies and explore their anti-tumor efficacy in future study.

In this study, our humanized h1B8 and h6D4 antibodies effectively suppressed cell proliferation and migration in a ROR1-dependent manner among lung, liver and breast cancer cells (Fig. 3). Cetin et al. reported the mRNA level

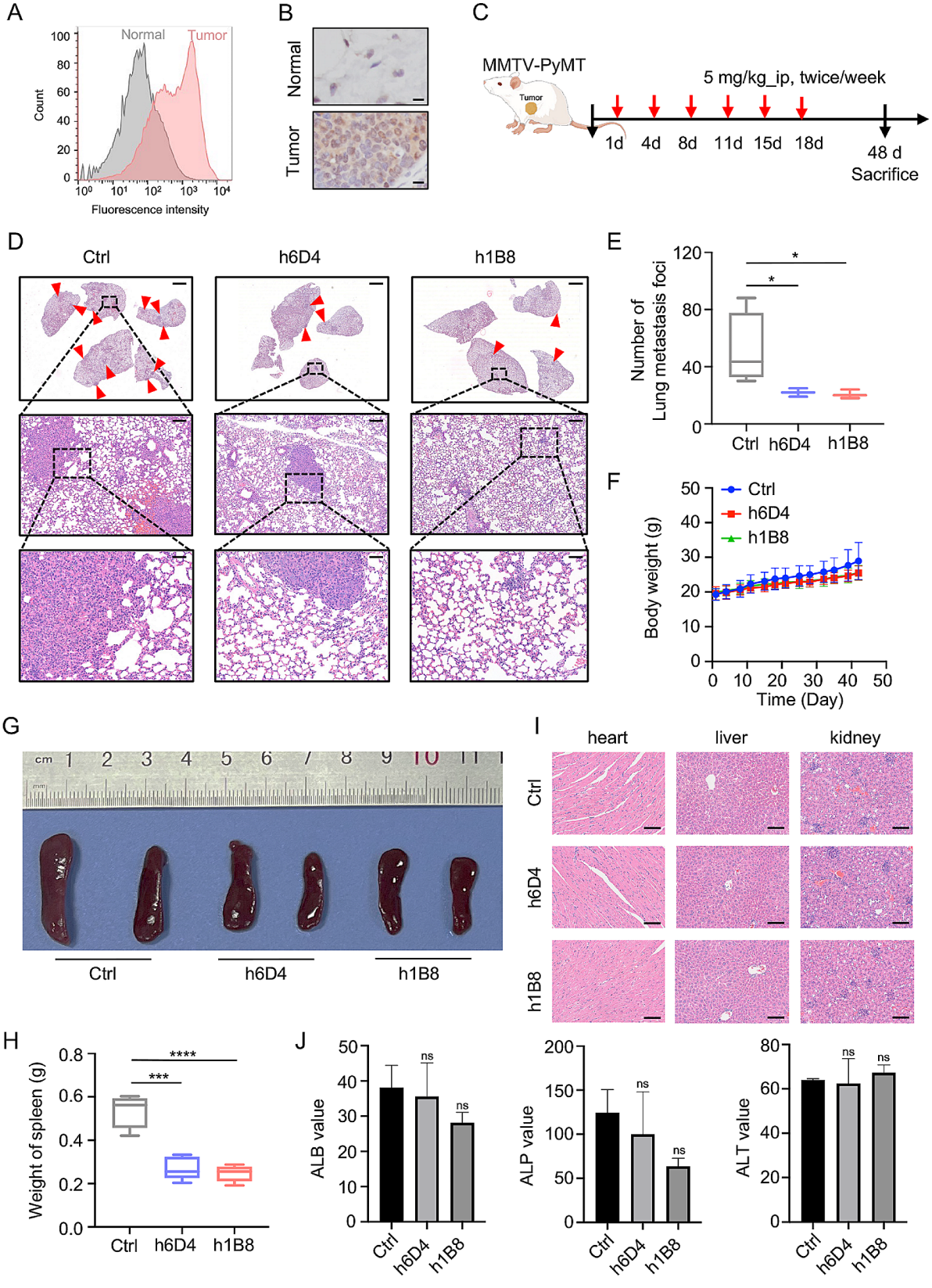

Fig. 6 (See legend on next page.)

(See figure on previous page.)

Fig. 6 Humanized h1B8 and h6D4 antibodies inhibit lung metastasis in the MMTV-PyMT breast cancer model. **(A-B)** ROR1 protein expression in breast tumors of mice was determined by flow cytometry **(A)** and immunohistochemistry assays **(B)**. Scale bar, 50 μm. **(C)** Schematic illustration of animal study. MMTV-PyMT mice were treated with anti-ROR1 antibodies (5 mg/kg) or the vehicle control, with injections given (twice a week, totally six times). **(D)** Representative H&E staining images of lung metastatic nodules from different groups of mice. Scale bar: Upper, 1 mm; Middle, 100 μm; Lower, 50 μm. **(E-F)** Lung metastatic foci **(E)** and body weights **(F)** of mice treated with or without anti-ROR1 antibodies. **(G-H)** Representative pictures **(G)** and weights **(H)** of spleens of mice treated with or without anti-ROR1 antibodies. **(I)** H&E staining images of major mouse organs. Scale bar, 50 μm. **(J)** Biochemical analyses of ALT, ALB, and ALP in the blood from different mice

of ROR1 is upregulated in hepatocellular carcinoma [34]. Here we confirmed the high expression of ROR1 at the protein level in HCC tissues (Fig. 1A). To the best of our knowledge, antibodies against ROR1 have not yet been reported in liver cancer, and our findings may provide a new option for targeted therapy of liver cancer. Increasing evidence demonstrates that ROR1 participates in various signaling pathways [35]. Notably, high expression of ROR1 positively correlates with AKT activation [36–38]. The link between ROR1 and AKT phosphorylation has been confirmed in multiple types of tumors. For example, the activation of AKT by ROR1 promotes the upregulation of cell cycle-related proteins in lung cancer cells, while inhibiting ROR1 signaling reduces the expression of CCNE1 and CDK4, two proteins involved in DNA synthesis and G1/S phase progression [39]. Additionally, AKT activation by ROR1 also accelerates cellular invasion process, impacting cell adhesion, movement, and migration in breast cancer, lung cancer, and melanoma [13, 36, 40]. Consistently, we found that treatment with humanized h1B8 and h6D4 antibodies in ROR1-positive A549, MDA-MB-231, and HCC-LM3 cells led to a significant decrease in phosphorylated AKT levels, while total AKT proteins remained unchanged. These results support that h1B8 and h6D4 antibodies exert their functions through blocking AKT signaling pathway. Besides WNT5A as a ROR1 ligand, IGFBP5 was recently identified to be another ligand for ROR1 [41]. Thus, it is interesting to investigate whether or not these two ligands are involved in AKT signaling when using h1B8 and h6D4 antibodies as molecular tools.

The anti-tumor effects of mAbs were usually evaluated in the immunodeficient mice. For instance, treatment with UC-961, an anti-ROR1 mAbs, significantly inhibits the growth of primary tumor-derived xenografts (PDXs) in immunodeficient mice [42]. Similarly, our humanized h1B8 and h6D4 antibodies exhibited good anti-tumor effects and no obvious toxicity in the lung cancer xenograft mice (immune deficiency) (Fig. 4). To evaluate the therapeutic effects of mAbs in a real tumor microenvironment, we chose two transgenic mouse models, the c-Myc/Alb-cre transgenic mice to develop liver cancer and the MMTV-PyMT transgenic mice to develop breast cancer [24, 43]. Our results from these two immunocompetent mouse models confirmed that humanized h1B8 and h6D4 antibodies have good anti-tumor effects without apparent toxicity (Figs. 5 and 6). Therefore, these two antibodies warrant further investigation for future application.

Although humanized h1B8 and h6D4 antibodies are promising for cancer therapy, this study has several limitations. Firstly, our anti-ROR1 antibodies exhibited high specificity and affinity to ROR1 protein, but the specific binding sites remain unknown. We will employ the cryo-electron microscopy technology to address this issue. Secondly, humanized h1B8 and h6D4 antibodies can effectively block AKT signaling pathway, but the anti-tumor pharmacological mechanisms of these antibodies need to be comprehensively dissected in future.

Conclusions

We successfully developed two humanized anti-ROR1 monoclonal antibodies, h1B8 and h6D4, with high specificity of ROR1 protein. Moreover, these two antibodies demonstrated effective anti-tumor activities in different mouse tumor models. Therefore, anti-ROR1 antibody-based therapy is a promising treatment strategy for ROR1-overexpressing tumors.

Abbreviation

ADCC	Antibody-dependent cell-mediated cytotoxicity
ADCs	Antibody-drug conjugates
ALB	Albumin
ALP	Alkaline phospholipase
ALT	Alanine aminotransferase
CAR-T	Chimeric antigen receptor T
CDR	Complementarity-determining region
ECD	Extracellular domain
FR	Framework region
HCC	Hepatocellular carcinoma
H&E	Hematoxylin and eosin
IHC	Immunohistochemistry
K_D	Equilibrium dissociation constant
mAbs	Monoclonal antibodies
PDXs	Patient-derived xenografts
ROR1	Receptor tyrosine kinase-like orphan receptor 1
SPR	Surface plasmon resonance

Supplementary Information

The online version contains supplementary material available at https://doi.org/10.1186/s12943-024-02075-y.

Supplementary Material 1

Acknowledgements

Authors would like to thank Ms. Jingyao Zhang in the Core Research Facilities of West China Hospital, Sichuan University, for her kind and professional helps with the SPR assays.

Author contributions
Y.P. conceived the project and designed the experiments; R.W., X.L., J.L., X.M. and Y.M. performed experiments; R.W., X.L. and J.L. analyzed data; and R.W., X.L. and Y.P. wrote the paper. All authors reviewed the manuscript.

Funding
This study was surppoted by National Natural Science Foundation of China (81821002) and the 1.3.5 Project for Disciplines of Excellence, West China Hospital, Sichuan University (ZYGD23027).

Data availability
No datasets were generated or analysed during the current study.

Declarations

Consent for publication
All authors have consented to submit this article for publication.

Competing interests
Y.P., R.W., X.L., and J.L. have filed patents related to this study. The other authors declare no competing interests.

Ethical approval and consent to participate
All mouse experiment procedures in this study were approved by the Institutional Animal Care and Use Committee of West China Hospital, Sichuan University.

Received: 12 June 2024 / Accepted: 29 July 2024
Published online: 13 August 2024

References

1. Green JL, Kuntz SG, Sternberg PW. Ror receptor tyrosine kinases: orphans no more. Trends Cell Biol. 2008;18:536–44.
2. Matsuda T, Nomi M, Ikeya M, Kani S, Oishi I, Terashima T, et al. Expression of the receptor tyrosine kinase genes, Ror1 and Ror2, during mouse development. Mech Dev. 2001;105:153–6.
3. Balakrishnan A, Goodpaster T, Randolph-Habecker J, Hoffstrom BG, Jalikis FG, Koch LK, et al. Analysis of ROR1 protein expression in human cancer and normal tissues. Clin Cancer Res. 2017;23:3061–71.
4. Cui B, Ghia EM, Chen L, Rassenti LZ, DeBoever C, Widhopf GF 2, et al. High-level ROR1 associates with accelerated disease progression in chronic lymphocytic leukemia. Blood. 2016;128:2931–40.
5. Zheng YZ, Ma R, Zhou JK, Guo CL, Wang YS, Li ZG, et al. ROR1 is a novel prognostic biomarker in patients with lung adenocarcinoma. Sci Rep. 2016;6:36447.
6. Zhou JK, Zheng YZ, Liu XS, Gou Q, Ma R, Guo CL, et al. ROR1 expression as a biomarker for predicting prognosis in patients with colorectal cancer. Oncotarget. 2017;8:32864–72.
7. Liu Y, Yang H, Chen T, Luo Y, Xu Z, Li Y, et al. Silencing of receptor tyrosine kinase ROR1 inhibits tumor-cell proliferation via PI3K/AKT/mTOR signaling pathway in lung adenocarcinoma. PLoS ONE. 2015;10:e0127092.
8. Yamaguchi T, Yanagisawa K, Sugiyama R, Hosono Y, Shimada Y, Arima C, et al. NKX2-1/TITF1/TTF-1-Induced ROR1 is required to sustain EGFR survival signaling in lung adenocarcinoma. Cancer Cell. 2012;21:348–61.
9. Yamaguchi T, Lu C, Ida L, Yanagisawa K, Usukura J, Cheng J, et al. ROR1 sustains caveolae and survival signalling as a scaffold of cavin-1 and caveolin-1. Nat Commun. 2016;7:10060.
10. Cui B, Zhang S, Chen L, Yu J, Widhopf GF 2nd, Fecteau JF, et al. Targeting ROR1 inhibits epithelial-mesenchymal transition and metastasis. Cancer Res. 2013;73:3649–60.
11. Zhang S, Chen L, Cui B, Chuang HY, Yu J, Wang-Rodriguez J, et al. ROR1 is expressed in human breast cancer and associated with enhanced tumor-cell growth. PLoS ONE. 2012;7:e31127.
12. Luo D, Qiu X, Zheng Q, Ming Y, Pu W, Ai M, et al. Discovery of novel receptor tyrosine kinase-like orphan receptor 1 (ROR1) inhibitors for cancer treatment. J Med Chem. 2024;67:10655–86.
13. Liu X, Pu W, He H, Fan X, Zheng Y, Zhou JK, et al. Novel ROR1 inhibitor ARI-1 suppresses the development of non-small cell lung cancer. Cancer Lett. 2019;458:76–85.
14. Zhang S, Zhang H, Ghia EM, Huang J, Wu L, Zhang J, et al. Inhibition of chemotherapy resistant breast cancer stem cells by a ROR1 specific antibody. Proc Natl Acad Sci U S A. 2019;116:1370–7.
15. Daneshmanesh AH, Hojjat-Farsangi M, Khan AS, Jeddi-Tehrani M, Akhondi MM, Bayat AA, et al. Monoclonal antibodies against ROR1 induce apoptosis of chronic lymphocytic leukemia (CLL) cells. Leukemia. 2012;26:1348–55.
16. Vaisitti T, Arruga F, Vitale N, Lee TT, Ko M, Chadburn A, et al. ROR1 targeting with the antibody-drug conjugate VLS-101 is effective in Richter syndrome patient-derived xenograft mouse models. Blood. 2021;137:3365–77.
17. Srivastava S, Furlan SN, Jaeger-Ruckstuhl CA, Sarvothama M, Berger C, Smythe KS, et al. Immunogenic chemotherapy enhances recruitment of CAR-T cells to lung tumors and improves antitumor efficacy when combined with checkpoint blockade. Cancer Cell. 2021;39:193–208. e10.
18. Srivastava S, Salter AI, Liggitt D, Yechan-Gunja S, Sarvothama M, Cooper K, et al. Logic-gated ROR1 chimeric antigen receptor expression rescues T cell-mediated toxicity to normal tissues and enables selective tumor targeting. Cancer Cell. 2019;35:489–503. e8.
19. Choi MY, Widhopf GF 2nd, Wu CC, Cui B, Lao F, Sadarangani A, et al. Preclinical specificity and safety of UC-961, a first-in-class monoclonal antibody targeting ROR1. Clin Lymphoma Myeloma Leuk. 2015;15:S167–9.
20. Choi MY, Widhopf GF 2nd, Ghia EM, Kidwell RL, Hasan MK, Yu J, et al. Phase I trial: Cirmtuzumab inhibits ROR1 signaling and stemness signatures in patients with chronic lymphocytic leukemia. Cell Stem Cell. 2018;22:951–9. e3.
21. Borcherding N, Kusner D, Liu GH, Zhang W. ROR1, an embryonic protein with an emerging role in cancer biology. Protein Cell. 2014;5:496–502.
22. Jones PT, Dear PH, Foote J, Neuberger MS, Winter G. Replacing the complementarity-determining regions in a human antibody with those from a mouse. Nature. 1986;321:522–5.
23. Scott AM, Wolchok JD, Old LJ. Antibody therapy of cancer. Nat Rev Cancer. 2012;12:278–87.
24. Mei Y, Zhou C, Liang CY, Lu GM, Zeng MS, Wang JJ, et al. A method to establish a c-Myc transgenic mouse model of hepatocellular carcinoma. MethodsX. 2020;7:100921.
25. Kipps TJ. ROR1: an orphan becomes apparent. Blood. 2022;140:1583–91.
26. Gura T. Therapeutic antibodies: magic bullets hit the target. Nature. 2002;417:584–6.
27. Adams GP, Weiner LM. Monoclonal antibody therapy of cancer. Nat Biotechnol. 2005;23:1147–57.
28. Castelli MS, McGonigle P, Hornby PJ. The pharmacology and therapeutic applications of monoclonal antibodies. Pharmacol Res Perspect. 2019;7:e00535.
29. Rezaei M, Ghaderi A. Monoclonal antibody production against vimentin by whole cell immunization in a mouse model. Iran J Biotechnol. 2018;16:e1802.
30. Gruber R, van Haarlem LJ, Warnaar SO, Holz E, Riethmuller G. The human antimouse immunoglobulin response and the anti-idiotypic network have no influence on clinical outcome in patients with minimal residual colorectal cancer treated with monoclonal antibody CO17-1A. Cancer Res. 2000;60:1921–6.
31. Haryadi R, Ho S, Kok YJ, Pu HX, Zheng L, Pereira NA, et al. Optimization of heavy chain and light chain signal peptides for high level expression of therapeutic antibodies in CHO cells. PLoS ONE. 2015;10:e0116878.
32. Carter PJ, Lazar GA. Next generation antibody drugs: pursuit of the 'high-hanging fruit'. Nat Rev Drug Discov. 2018;17:197–223.
33. Jin Y, Schladetsch MA, Huang X, Balunas MJ, Wiemer AJ. Stepping forward in antibody-drug conjugate development. Pharmacol Ther. 2022;229:107917.
34. Cetin M, Odabas G, Douglas LR, Duriez PJ, Balcik-Ercin P, Yalim-Camci I, et al. ROR1 expression and its functional significance in hepatocellular carcinoma cells. Cells. 2019;8:210.
35. Quezada MJ, Lopez-Bergami P. The signaling pathways activated by ROR1 in cancer. Cell Signal. 2023;104:110588.
36. Fernandez NB, Lorenzo D, Picco ME, Barbero G, Dergan-Dylon LS, Marks MP, et al. ROR1 contributes to melanoma cell growth and migration by regulating N-cadherin expression via the PI3K/Akt pathway. Mol Carcinog. 2016;55:1772–85.
37. Hojjat-Farsangi M, Khan AS, Daneshmanesh AH, Moshfegh A, Sandin A, Mansouri L, et al. The tyrosine kinase receptor ROR1 is constitutively phosphorylated in chronic lymphocytic leukemia (CLL) cells. PLoS ONE. 2013;8:e78339.
38. Daneshmanesh AH, Hojjat-Farsangi M, Moshfegh A, Khan AS, Mikaelsson E, Osterborg A, et al. The PI3K/AKT/mTOR pathway is involved in direct apoptosis of CLL cells induced by ROR1 monoclonal antibodies. Br J Haematol. 2015;169:455–8.

39. Zhou Q, Zhou S, Wang H, Li Y, Xiao X, Yang J. Stable silencing of ROR1 regulates cell cycle, apoptosis, and autophagy in a lung adenocarcinoma cell line. Int J Clin Exp Pathol. 2020;13:1108–20.
40. Pandey G, Borcherding N, Kolb R, Kluz P, Li W, Sugg S et al. ROR1 potentiates FGFR signaling in basal-like breast Cancer. Cancers (Basel). 2019;11.
41. Lin W, Niu R, Park SM, Zou Y, Kim SS, Xia X, et al. IGFBP5 is an ROR1 ligand promoting glioblastoma invasion via ROR1/HER2-CREB signaling axis. Nat Commun. 2023;14:1578.
42. Zhang S, Cui B, Lai H, Liu G, Ghia EM, Widhopf GF 2, et al. Ovarian cancer stem cells express ROR1, which can be targeted for anti-cancer-stem-cell therapy. Proc Natl Acad Sci U S A. 2014;111:17266–71.
43. Guy CT, Cardiff RD, Muller WJ. Induction of mammary tumors by expression of polyomavirus middle T oncogene: a transgenic mouse model for metastatic disease. Mol Cell Biol. 1992;12:954–61.

Publisher's Note

Springer Nature remains neutral with regard to jurisdictional claims in published maps and institutional affiliations.